

Th.E. Labrujère, R.A. Maarsingh and J. Smith
 National Aerospace Laboratory (NLR)
 Amsterdam, The Netherlands

Abstract

The present paper describes two alternative correction methods for wall interference based on measured boundary conditions. In both methods it is assumed that at or near the tunnel boundary the flow velocity will be measured in magnitude and direction and that the main part of the flow field may be considered irrotational and subsonic. One method aims at a correction in terms of changes in free stream velocity and angle of attack. The other method aims at corrections of the velocity distribution along the model. The application of both methods is demonstrated numerically for the case of a single and a multiple airfoil in a solid wall test section.

Symbols

| | |
|----------------|---|
| c | airfoil chord |
| n | normal to the flow boundary (directed inwards) |
| r | distance between two points (x,y) and (ξ,η) |
| s,t | arclength measured along the flow boundary |
| u,v | disturbance velocity components in x and y direction respectively |
| x,y | Cartesian axis system |
| C _l | lift coefficient |
| C _p | pressure coefficient |
| D | flowdomain |
| H | tunnel height |
| Q | dynamic pressure |
| U,V | velocity components in x and y direction |
| α | angle of attack |
| Δ | difference |
| φ | disturbance velocity potential |
| φ | velocity potential |
| σ | boundary of flow domain |
| ξ,η | integration variables corresponding with x and y respectively |

Subscripts

| | |
|-----|--|
| i | refers to reference point for determination of global wall influence |
| m | refers to mid-chord |
| ref | refers to undisturbed tunnel flow |
| ∞ | refers to undisturbed free flow |
| C | refers to correction |
| F | refers to free air |
| M | refers to the model |
| T | refers to the tunnel |
| W | refers to the walls |

1. Introduction

In line with modern developments in wind tunnel wall correction methods, work is in progress at NLR for the development of a method based on measured boundary conditions. A fairly simple and fast calculation method can be formulated⁽¹⁾ if it is assumed that the velocity distribution along the tunnel walls can be measured. This method is applicable in principle to experiments in subsonic and transonic flow, solid and ventilated wall wind tunnels, 2D as well as 3D.

Copyright © 1984 by ICAS and AIAA. All rights reserved.

From the velocity distribution along the walls, the wall induced perturbation velocity field can be determined under certain conditions applying Green's theorem. If the gradients of this perturbation field are small the wind tunnel influence can be determined in terms of a correction to the free stream velocity and the angle of attack. In general these gradients will be small if the wind tunnel model has a moderate size with respect to the dimensions of the wind tunnel e.g. in 2D for small values of c/H, where c is a characteristic length of the model and H is the height of the wind tunnel. Thus, assuming that in near future measurement techniques will be improved such that the velocity distribution along the tunnel walls can be measured, it will be possible to determine a sufficiently accurate correction for the majority of wind tunnel experiments.

However, situations may occur where the flow must be considered uncorrectable in this way e.g. in the case of airfoils with high lift devices at large angles of attack. Having met this difficulty, a limited numerical study of the latter case has been made at NLR. It appeared that the "uncorrectability" is due to the phenomenon of streamline curvature. The latter is taken into account in a very limited way only when applying a global correction method. This fact has been demonstrated with the aid of an inverse calculation method⁽²⁾ that is capable of determining the shape of a multi-element airfoil which produces a specified pressure distribution.

From this study it has been concluded that for the flows considered here, correction for wind tunnel wall influence would only be feasible if a method for local correction could be developed.

Kraft and Dahm⁽³⁾ have described an approach which may be used to derive such a method. Their method has the drawback that the airfoil is assumed to be thin and at low angle of attack such that a linearized perturbation approximation is valid. But this assumption allows the derivation of closed expressions for local correction in which the model geometry does not appear. As this assumption can not be made for the flow considered here, the approach of Kraft and Dahm had to be reformulated. This appeared to be possible though at the cost of introducing a model representation again.

The present paper gives a description of both global and local correction methods developed at NLR. The application of the methods is demonstrated numerically for the case of a single and multiple airfoil in a solid-wall test section.

2. Correction methods using measured boundary conditions

Flow problem

The correction methods presented here are both based on the assumption that at or near the tunnel boundary the flow velocity will be measured both in magnitude and direction. In case of solid walls,

measurement of the static pressure suffices to determine magnitude and direction, but in case of ventilated walls the flow direction will have to be measured explicitly.

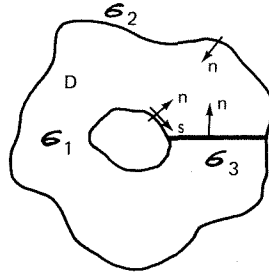
The key problem to be solved when considering wall influence is how to establish a relation between tunnel flow and free flow around a given model. Rather simple solutions to this problem can be formulated if it may be assumed that the flow or at least the greater part of the flow is irrotational and subsonic. With this assumption Goethert's rule may be applied in order to arrive at an equivalent incompressible flow problem. Then the wall influence problem reduces to the problem of relating the incompressible velocity potential ϕ_T of the flow in the tunnel to the incompressible velocity potential ϕ_F of free flow.

In order to solve this problem the flow situations as depicted in figure 1 are compared. The velocity potential in the tunnel is split in ϕ_{ref} due to undisturbed flow and ϕ_T due to the disturbance by the tunnel walls and the model. The potential of free flow is split up in ϕ_∞ due to undisturbed flow and ϕ_F due to the disturbance by the model. Infinite space is split up in three domains: a domain D_0 outside the tunnel walls, a domain D_T limited by σ_W at the outer side and by σ_M at the inner side and domain D_M inside σ_M .

The present methods are both based on application of Green's theorem. If the flow in a domain D has a cyclic velocity potential ϕ and r denotes the distance from any point in the flow domain to a fixed point P it can be derived that:

$$\int_{\sigma_1+\sigma_2} \left\{ \phi \frac{\partial}{\partial n} \ln r - \frac{\partial \phi}{\partial n} \ln r \right\} ds + \Delta \phi \int_{\sigma_3} \frac{\partial}{\partial n} \ln r ds =$$

$$= \begin{cases} 0 & \text{for } P \text{ outside } D \\ -\pi \phi(P) & \text{for } P \text{ on the boundary} \\ -2\pi \phi(P) & \text{for } P \text{ inside } D \end{cases} \quad (1)$$



where σ_1 and σ_2 form the boundary of the flow domain, σ_3 is the slit which is necessary to allow a cyclic potential and $\Delta \phi$ is the jump in potential across the slit.

Global correction method

The global correction method⁽¹⁾, following the approach as formulated by Ashill⁽⁴⁾, aims at the determination of corrections for tunnel wall influence in terms of changes in free stream velocity and angle of attack. The assumption of irrotational subsonic flow is made for a region outside a relatively small area around the model. So, the boundary σ_M in figure 1 does not necessarily coincide with the boundary of the model.

In order to be able to determine global corrections it is necessary to assume that, corresponding to the tunnel flow, there exists a free flow around the model such that the disturbances at σ_M in free flow and in tunnel flow are approximately the same,

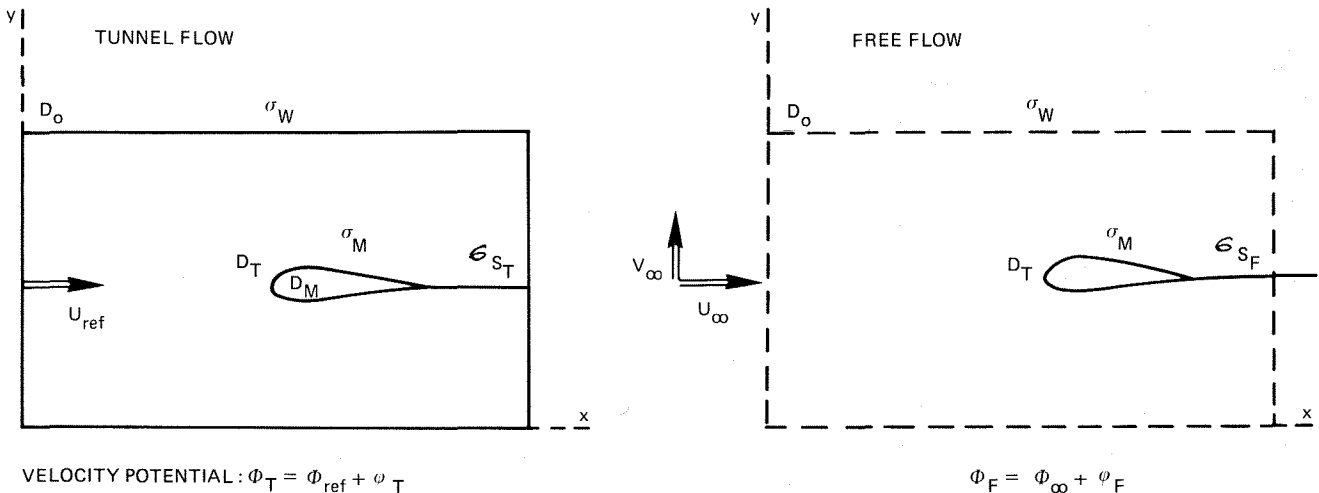


Fig. 1 The flowdomains

and that the lift in both flow situations is the same.

Furthermore it is assumed that the flowfield near the model in the tunnel is globally the same as in free air, such that at least in one suitably chosen point the velocity will be the same.

For convenience the present method will be formulated in terms of velocity components rather than the velocity potential. Considering the domain D_T (Fig. 1), applying Eq. (1) to $U = \frac{\partial \phi}{\partial x}$ in stead of ϕ and reminding that this function is single-valued throughout D_T , so that there is no jump in U across σ_{ST} , the velocity component:

$$U_T = U_{ref} + u_T \quad (2)$$

can be determined from

$$U_T = U_{ref} - \frac{1}{2\pi} \int_{\sigma_W} \left\{ u_T \frac{\partial}{\partial n} \ln r - \frac{\partial u_T}{\partial n} \ln r \right\} ds - \frac{1}{2\pi} \int_{\sigma_M} \left\{ u_T \frac{\partial}{\partial n} \ln r - \frac{\partial u_T}{\partial n} \ln r \right\} ds \quad (3)$$

for any point in D_T .

Applying the conditions of continuity and irrotational flow, this expression can by partial integration, be rewritten as:

$$U_T = U_{ref} - \frac{1}{2\pi} \int_{\sigma_W} \left\{ u_T \frac{\partial}{\partial n} \ln r + v_T \frac{\partial}{\partial s} \ln r \right\} ds - \frac{1}{2\pi} \int_{\sigma_M} \left\{ u_T \frac{\partial}{\partial n} \ln r + v_T \frac{\partial}{\partial s} \ln r \right\} ds \quad (4)$$

In free flow the velocity component

$$U_F = U_\infty + u_F \quad (5)$$

can be determined analogously from:

$$U_F = U_\infty - \frac{1}{2\pi} \int_{\sigma_M} \left\{ u_F \frac{\partial}{\partial n} \ln r + v_F \frac{\partial}{\partial s} \ln r \right\} ds \quad (6)$$

As has been stated above it is assumed that:

$$u_F \approx u_T \quad \text{and} \quad v_F \approx v_T \quad \text{at} \quad \sigma_M \quad (7)$$

Hence the second integral of Eq. (4) is approximately equal to the integral of Eq. (6).

Furthermore it is assumed that

$$U_F = U_T \quad \text{at some point in} \quad D_T \quad (8)$$

Thus from Eqs. (4) and (6) it follows that:

$$U_\infty - U_{ref} = \frac{-1}{2\pi} \int_{\sigma_W} \left\{ u_T \frac{\partial}{\partial n} \ln r + v_T \frac{\partial}{\partial s} \ln r \right\} ds = \Delta U \quad (9)$$

Analogously it can be derived that for the velocity component $V = \frac{\partial \phi}{\partial y}$:

$$V_\infty = - \frac{1}{2\pi} \int_{\sigma_W} \left\{ v_T \frac{\partial}{\partial n} \ln r - u_T \frac{\partial}{\partial s} \ln r \right\} ds = \Delta V \quad (10)$$

In this way corrections for the tunnel wall influence in terms of a correction to the free stream velocity and the angle of attack are determined by evaluating integrals along the tunnel walls in which the measured disturbance velocities u_T and v_T appear. Moreover, as the boundary σ_M does not appear in the ultimate expressions, there is no need to make any assumptions on the actual shape of D_M .

The values of ΔU and ΔV depend on the choice of the point where Eqs. (9) and (10) are evaluated.

Because the choice of this reference point is more or less arbitrary a reliable global correction is determined only if the gradients of the wall induced perturbation field are small; in other words if there is only a gradual variation of ΔU and ΔV .

If (x_i, y_i) denotes the reference point the actual corrections applied to the measured quantities are defined in more or less the classical way as follows:

$$\text{Incidence} \quad \alpha_C = \alpha_T + \frac{\Delta V}{U_{ref}} \quad (\text{radians}) \quad (11)$$

$$\text{Dynamic pressure} \quad Q_C = Q_T \left(1 + 2 \frac{\Delta U}{U_{ref}} \right) \quad (12)$$

$$\text{Lift} \quad Cl_C = Cl_T \frac{Q_T}{Q_C} + 2\pi \frac{d}{dx} \left(\frac{\Delta V}{U_{ref}} \right) (x_i - \frac{3}{4}c) \quad (13)$$

$$\text{Pressure coefficient} \quad C_{P_C} = C_{P_T} \frac{Q_T}{Q_C} + 2 \frac{\Delta U}{U_{ref}} \quad (14)$$

The applicability of the present method is examined to some extent by means of numerical examples in section 3.

Local correction method

The local correction method following an approach similar to that of Kraft and Dahm⁽³⁾ aims at correcting for tunnel wall influence in terms of changes in velocity distribution along the model rather than in terms of the onset flow conditions. Considering the irrotational subsonic flows as depicted in figure 1 again, this means that the undisturbed velocity potentials in both flow situations considered are chosen identical:

$$\phi_\infty = \phi_{ref} \quad (15)$$

From the condition of tangential flow at the model it follows that:

$$\text{in tunnel flow:} \quad \frac{\partial \phi_T}{\partial n} = \frac{\partial \phi_{ref}}{\partial n} + \frac{\partial \phi_T}{\partial n} = 0 \quad (16)$$

$$\text{in free flow:} \quad \frac{\partial \phi_F}{\partial n} = \frac{\partial \phi_\infty}{\partial n} + \frac{\partial \phi_F}{\partial n} = \frac{\partial \phi_{ref}}{\partial n} + \frac{\partial \phi_F}{\partial n} = 0 \quad (17)$$

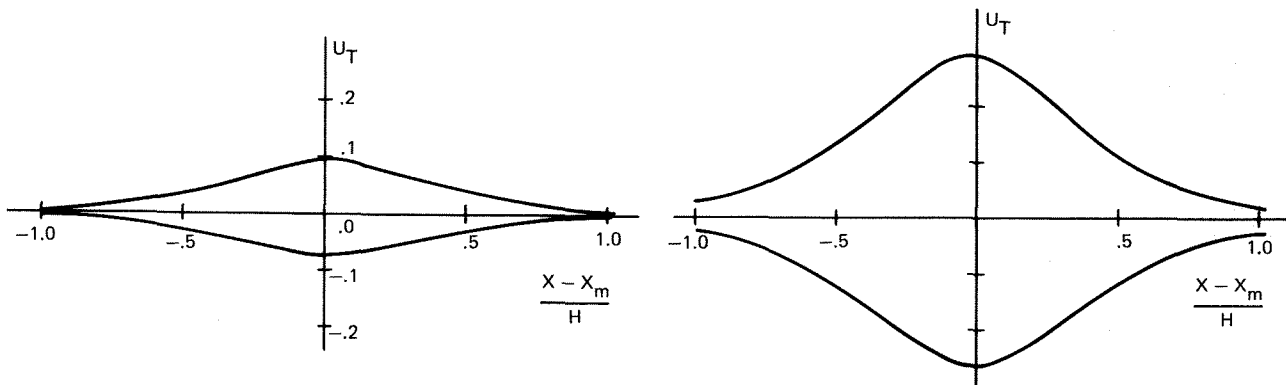
$$\text{So:} \quad \frac{\partial \phi_T}{\partial n} = \frac{\partial \phi_F}{\partial n} \quad \text{at the model} \quad (18)$$

According to Eq. (1) there holds for a point P at the model in tunnel flow:

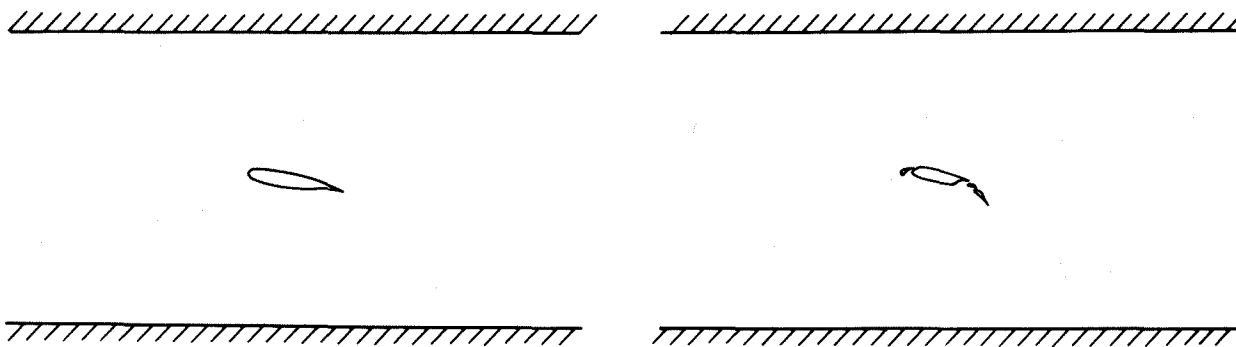
$$\begin{aligned} \phi_T(P) = \phi_{ref}(P) - \frac{1}{\pi} \int_{\sigma_W} \left\{ \omega_T \frac{\partial}{\partial n} \ln r - \frac{\partial \phi_T}{\partial n} \ln r \right\} ds \\ - \frac{1}{\pi} \int_{\sigma_M} \left\{ \omega_T \frac{\partial}{\partial n} \ln r - \frac{\partial \phi_T}{\partial n} \ln r \right\} ds \\ - \frac{1}{\pi} \Delta \phi_T \int_{\sigma_{ST}} \frac{\partial}{\partial n} \ln r \, ds \end{aligned} \quad (19)$$

and for a point P at the model in free flow:

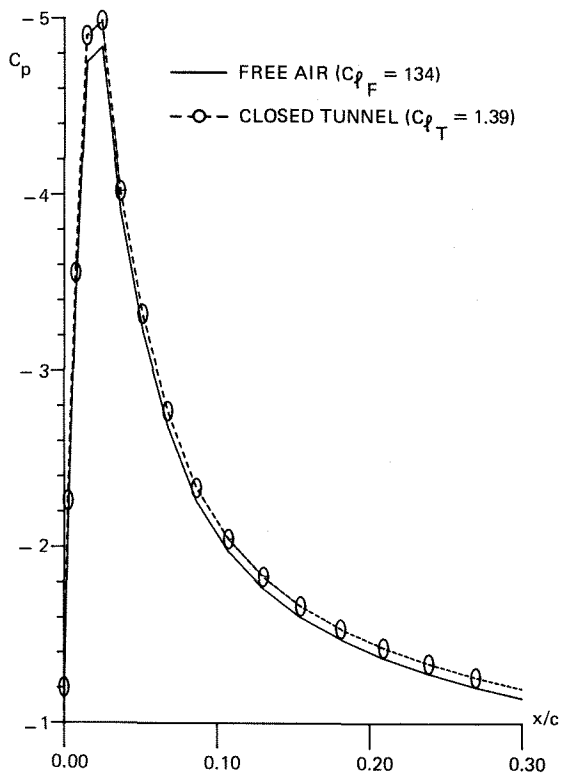
$$\begin{aligned} \phi_F(P) = \phi_\infty(P) - \frac{1}{\pi} \int_{\sigma_M} \left\{ \omega_F \frac{\partial}{\partial n} \ln r - \frac{\partial \phi_F}{\partial n} \ln r \right\} ds \\ - \frac{1}{\pi} \Delta \phi_F \int_{\sigma_{SF}} \frac{\partial}{\partial n} \ln r \, ds \end{aligned} \quad (20)$$



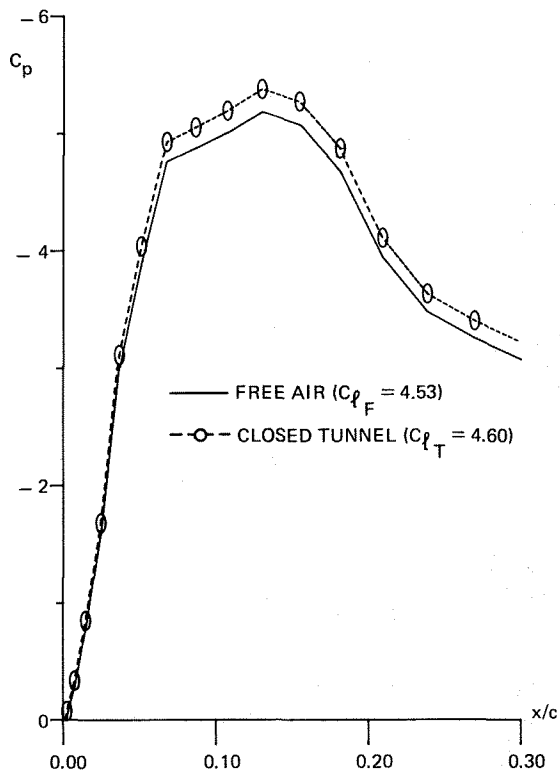
DISTURBANCE VELOCITY DISTRIBUTION ALONG THE TUNNEL WALLS



CONFIGURATIONS CONSIDERED



PRESSURE DISTRIBUTION ON THE UPPER SIDE OF THE AIRFOIL



PRESSURE DISTRIBUTION ON THE UPPER SIDE OF THE MAIN AIRFOIL ELEMENT

Fig. 2 Numerically simulated flow in free air and closed wall wind tunnel

Although not really essential, it is presumed for simplicity that the test section is sufficiently long so that the difference between the integrals over σ_{ST} and σ_{SF} is negligible. Then from subtraction of Eqs. (19) and (20) it follows with Eqs. (15) and (18):

$$\begin{aligned} \phi_C(P) + \frac{1}{\pi} \int \phi_C \frac{\partial}{\partial n} \ln r \, ds + \frac{1}{\pi} \Delta\phi_C \int \frac{\partial}{\partial n} \ln r \, ds = \\ - \frac{1}{\pi} \int \left\{ \frac{\partial \phi_T}{\partial n} \ln r - \frac{\partial \phi_F}{\partial n} \ln r \right\} ds \end{aligned} \quad (21)$$

$$\text{where} \quad \phi_C = \phi_T - \phi_F = \phi_T - \phi_F \quad (22)$$

By means of partial integration the right-hand side term of Eq. (21) is rewritten:

$$\begin{aligned} - \frac{1}{\pi} \int \left\{ \phi_T \frac{\partial}{\partial n} \ln r - \frac{\partial \phi_T}{\partial n} \ln r \right\} ds = - Cl_T c \\ - \frac{1}{\pi} \int \left\{ \frac{\partial \phi_T}{\partial s} \tan^{-1} \frac{y-\eta}{x-\xi} - \frac{\partial \phi_T}{\partial n} \ln r \right\} ds \end{aligned} \quad (23)$$

where Cl_T is the measured lift coefficient. Thus, the right hand side term is determined from the measured velocity distribution along the tunnel wall and at the model and Eq. (21) establishes an integral equation for the correction potential ϕ_C . Applying the Kutta condition of smooth flow at the trailing edge of the airfoil, this equation is solved by means of a panel method developed at NLR⁽²⁾. Differentiation of Eq. (21) establishes an expression for the tangential derivative of ϕ_C :

$$\begin{aligned} \frac{\partial \phi_C}{\partial t} = - \frac{1}{\pi} \int \left\{ \frac{\partial \phi_C}{\partial s} \frac{\partial}{\partial t} \tan^{-1} \frac{y-\eta}{x-\xi} \, ds \right. \\ \left. - \frac{1}{\pi} \int \left\{ \frac{\partial \phi_T}{\partial s} \frac{\partial}{\partial t} \tan^{-1} \frac{y-\eta}{x-\xi} - \frac{\partial \phi_T}{\partial n} \frac{\partial}{\partial t} \ln r \right\} ds \right. \end{aligned} \quad (24)$$

by means of which a correction to the measured tangential velocity is determined.

In contrast with the previously described method, the present method makes use of detailed information about the model considered. However, whereas the previous method can only lead to an approximation of the free flow, the present method leads to an "exact" description of the free flow within the limits set by the accuracy of measurement and computation. This will be demonstrated by means of numerical examples in the next section.

3. Discussion of results

In order to evaluate the methods described above with respect to the concepts of global and local correction a numerical demonstration was performed. To this end a panel method⁽²⁾ was applied for the determination of the flow around a single airfoil and a multiple airfoil (see Fig. 2) in a closed wall wind tunnel as well as in free air. The tunnel walls were located at ± 2 chords from the airfoil in order to obtain a realistic chord over tunnelheight ratio ($c/H = .25$). As may be seen from figure 2 the wall-influence on the pressure distribution is of the same order of magnitude in both cases. The "measured" velocity distribution along the tunnel walls (as depicted in Fig. 2) was substituted in Eqs. (9) through (14) to determine global corrections and into Eq. (21) through (24) to determine local corrections.

Global corrections

As has been stated before, the tunnel influence corrections that are determined by means of the global correction method depend on the choice of the reference point where Eqs. (9) and (10) are evaluated. So the method can only be applied successfully if this choice is of minor importance.

Fig. 3 shows the distribution of the wall interference velocities along the test section centre line for both test cases. In both cases the variation of ΔU is very small. So, it may be expected that the correction for blockage may be performed equally

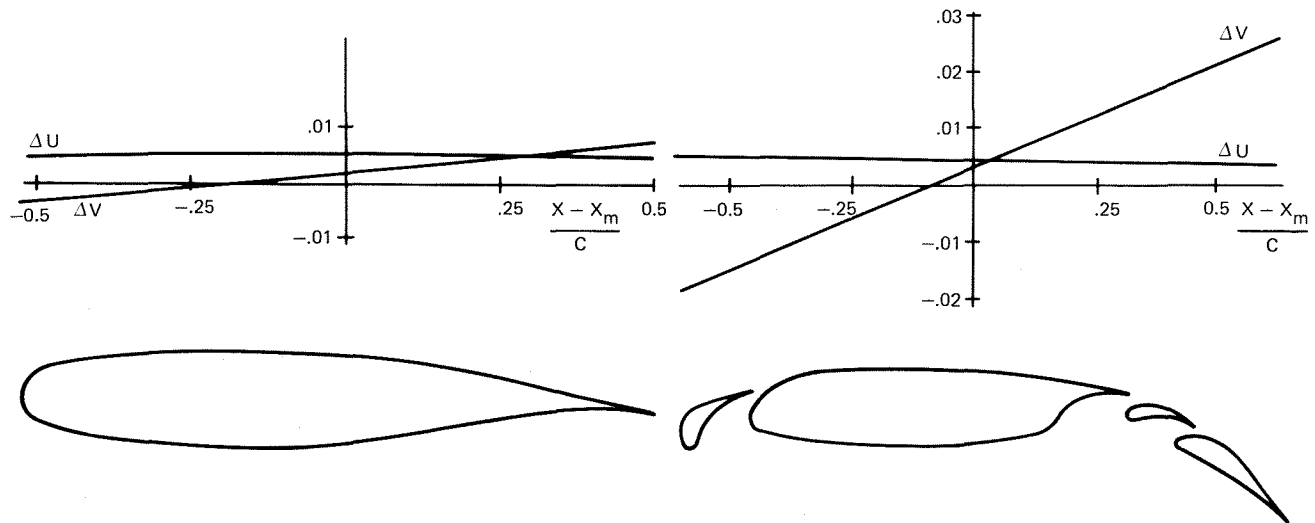


Fig. 3 Distribution of wall interference velocities along the test section centre line

well in both cases. However, the gradient of the upwash variation is much larger for the high lift configuration than for the single airfoil.

Choosing the mid-chord point (x_m, y_m) as reference point for the determination of ΔU and ΔV , the wall corrections have been calculated in terms of a corrected angle of attack and lift coefficient as well as a corrected pressure distribution. A calculation by means of the panel method for the configuration in free air at the corrected angle of attack provides an easy verification of the corrections performed. The following table gives a comparison of angle of attack and lift coefficient, while figure 4 presents a comparison of the calculated pressure distributions.

| | α_T | Cl_T | α_C | Cl_C | α_F | Cl_F |
|-----------------|------------|--------|------------|--------|------------|--------|
| single airfoil | 8.0 | 1.39 | 8.11 | 1.36 | 8.11 | 1.36 |
| high lift conf. | 8.0 | 4.60 | 8.14 | 4.51 | 8.14 | 4.55 |
| | Tunnel | | Corrected | | Free air | |

From the table it appears that the "free air solution" obtained by means of global correction is correct for the single airfoil, while figure 4 shows that also the pressure distribution is in close agreement with the true solution. The correction for the high lift configuration however, is overestimated as far as the total lift coefficient is concerned. The corrections to the pressure distribution are found to be overestimated for slat and flap and underestimated for the main element.

As has been remarked before, the value of the global corrections depends on the location of the reference point. In order to examine the effect of this choice, different corrected lift coefficients and angles of attack have been determined for different locations of the reference point. In figure 5 the $Cl-\alpha$ curves thus determined are compared with the free air solutions. For the single airfoil there is a close agreement between the two curves which implies that the global correction is practically independent of the choice of the reference point. For the high lift configuration the two curves differ considerably. Their point of intersection corresponds with a reference point located about half a chord upstream from the airfoil. Corrections calculated by means of this point lead to $\alpha_C = 6.2$ and $Cl_C = 4.29$.

Though the high lift configuration in free air has indeed this lift coefficient at this angle of attack, there is hardly any agreement between the globally corrected and free air pressure distributions, as is illustrated by figure 6.

Thus, apparently the high lift case has to be considered uncorrectable by the global method.

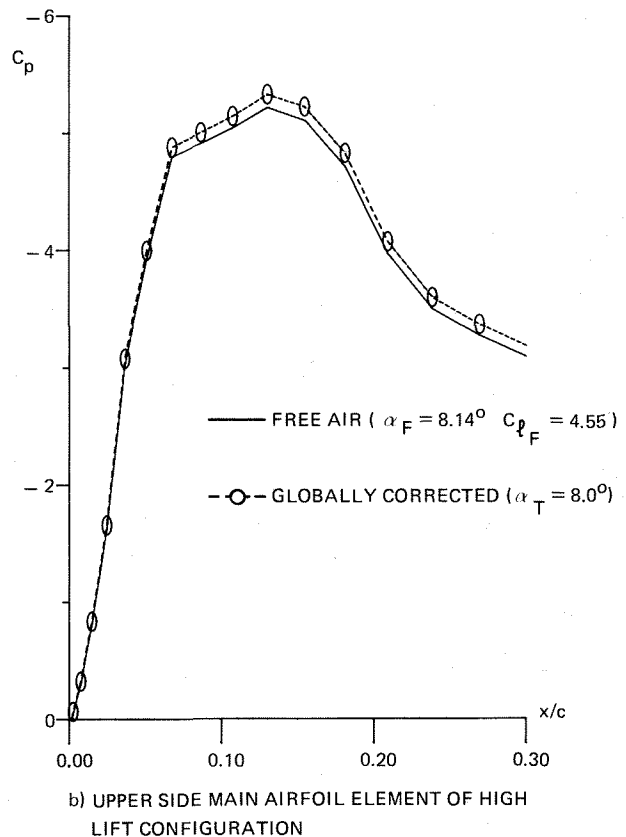
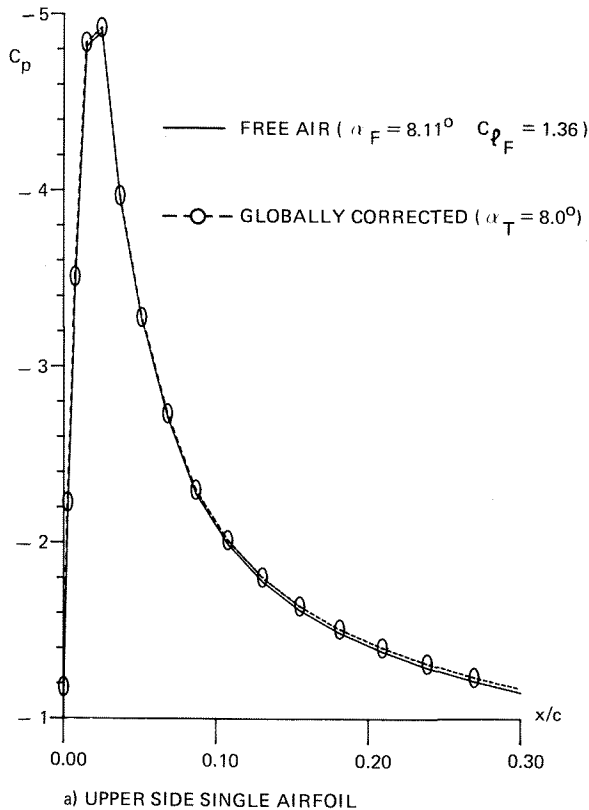


Fig. 4 Globally corrected pressure distributions compared with free air pressure distributions at the corrected angle of attack

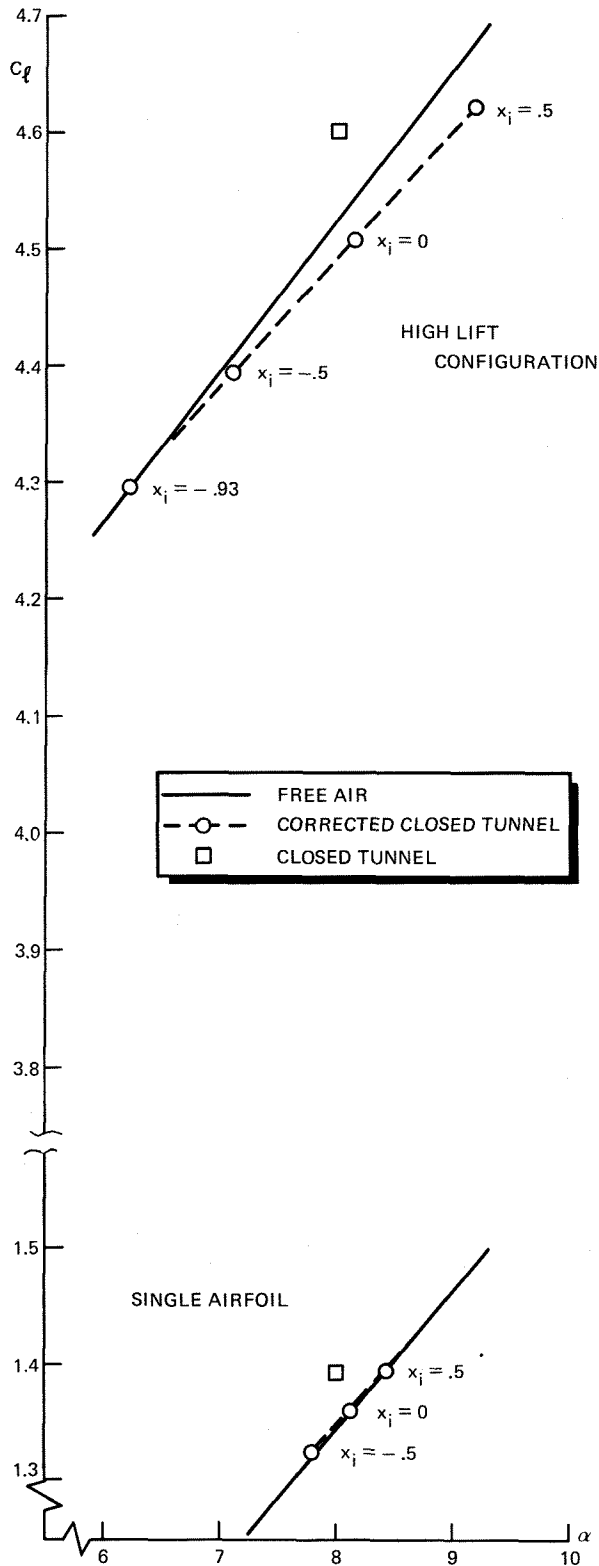


Fig. 5 Globally corrected lift coefficient determined by different choices of the reference point (indicated by x_i) compared with the free air solution

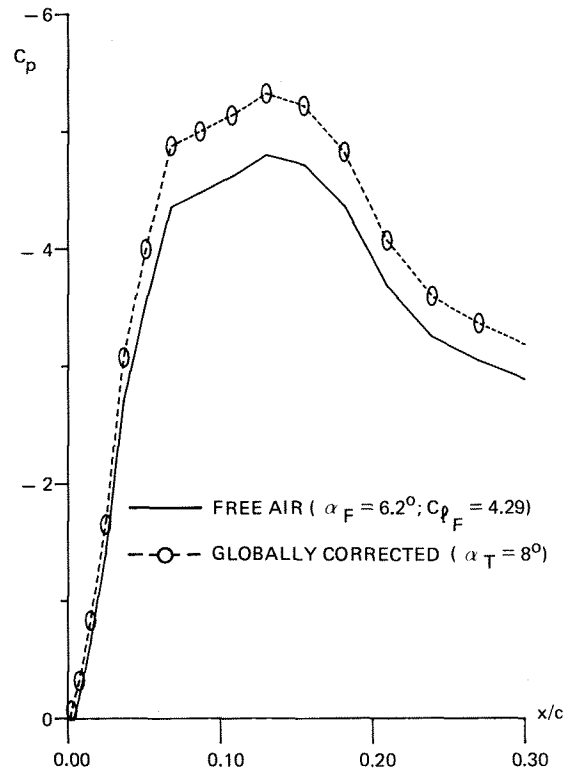


Fig. 6 Globally corrected pressure distribution compared with a free air pressure distribution which has the same lift coefficient as obtained by means of global correction

Model adaptation

The uncorrectability of the high lift case is obviously due to the large variation of the wall-induced upwash. This part of the wall influence is often interpreted as a virtual modification of the camber of the model, which suggests that the agreement between free air and tunnel flow might be improved by modifying the deflection angles of slat, vane and flap.

To investigate this the design method for multiple airfoils⁽²⁾ developed at NLR has been applied. This design method is capable of designing an airfoil such that it will produce, in free air, a specified pressure distribution.

So, the pressure distribution determined for tunnel flow was prescribed as the pressure distribution to be produced by the modified airfoil in free air. In order to keep the interpretation of the results as simple as possible, the design method was applied such that the relative positions of the airfoil elements were modified, while the shape of the elements was kept fixed.

The result of the design process is shown in figure 7 where the original and modified configurations are compared. Calculation of the flow around the modified configuration in free air showed that this configuration produces indeed the same lift coefficient as the original configuration in tunnel

flow. The pressure distributions as shown in figure 8 for the main element are, of course, not exactly the same because of effects such as blockage that have not been taken into account and because of the limited extent of the modification. However, the camber effect of wall interference is clearly demonstrated.

This example shows that strong curvature effects may be interpreted as corrections to slat and flap angles. However, from the point of view of interpretation of wind tunnel measurements this seems rather unattractive. Moreover, determining the corrections requires the use of a design method which makes this procedure unattractive for routine application.

Local corrections

For the present examples it is also possible to eliminate the tunnel wall influence completely from the pressure distribution measured in the tunnel. From the measured velocity distribution along the tunnel walls the correction potential at the airfoil contour is calculated to subsequently correct the model velocity distribution. The resulting pressure distribution for the main element of the high lift configuration is presented in figure 9. Because of the fact that the example considered here is trivial in the sense that it satisfies all assumptions underlying the present method, the corrected pressure distribution practically coincides with the pressure distribution on the model in free air. The differences which are hardly visible, are due to computational imperfections.

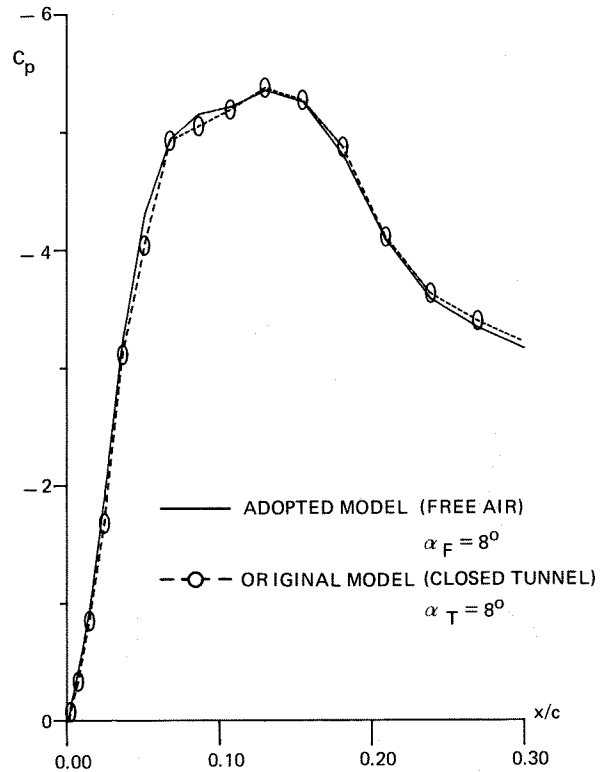


Fig. 8 Pressure distributions on the main element of the adapted configuration in free air and the original configuration in closed tunnel

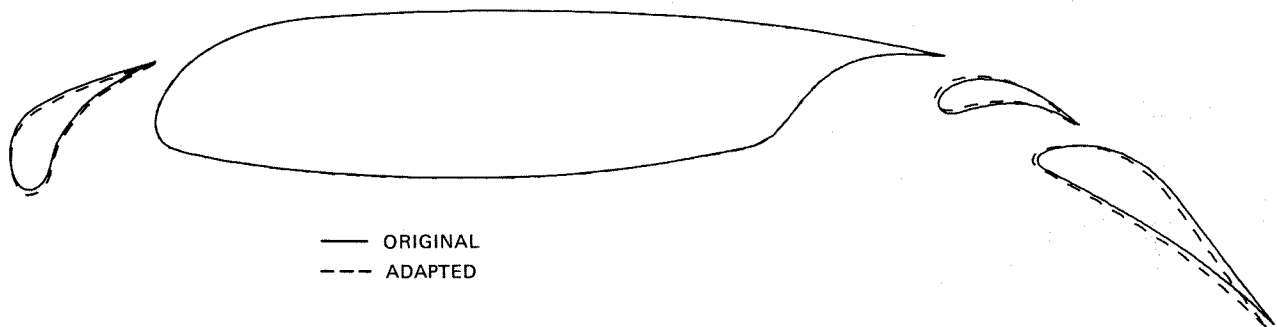


Fig. 7 Model adaptation for simulation of wall interference

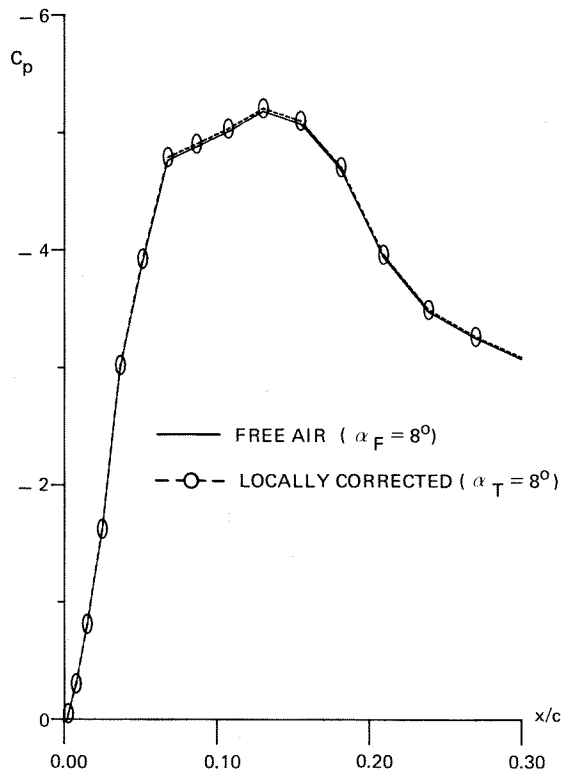


Fig. 9 Locally corrected pressure distribution compared with free air pressure distribution

4. Concluding remarks

Two types of wall correction methods using measured boundary conditions have been described. The global correction method is by far the most attractive. It does not need any kind of model representation, the computation is very fast because it requires the evaluation of two integrals only and moreover it seems applicable to a wide variety of wind tunnel experiments 2D as well as 3D. Generally speaking a global correction method is applicable if the flow around the model in the tunnel is not essentially different from the flow in the air, in other words if the flow phenomena observed in the tunnel may be considered as free air flow phenomena if at somewhat different onset flow conditions.

Situations may occur where the difference between the tunnel flow and the free air flow becomes too large. As has been demonstrated such a situation is met if the wall induced upwash variation is too large. Then the determination of a correction in terms of angle of attack becomes impossible.

By means of a computational design method it has been shown that the upwash variation may be interpreted as changes in the model geometry. This, however, seems a rather inconvenient way of correcting routinely for wall influence.

The application of local corrections seems more satisfying, in case of large upwash gradients. For irrotational subsonic flow, such a correction

method can be formulated straight forwardly, though at the cost of a detailed representation of the model. The local correction method involves the application of a panel method and thus requires more computation time than the global correction method. But as the application of panel methods is a matter of routine nowadays, even for 3D, this should not be prohibitive. More important is the restriction to irrotational subsonic flow. Moreover, the method is not applicable in transonic flows where non linear effects are important. The inclusion of viscous effects, however, by means of boundary layer calculation methods should not be a problem.

5. References

1. Labrujère, Th.E. Correction for wall influence by means of a measured boundary condition method. (To be published)
2. Labrujère, Th.E. MAD, a system for computer aided analysis and design of multi-element airfoils. NLR TR 83136 L (1983)
3. Kraft, E.M. and Dahn, W.J.A. Direct assessment of wall interference in a two-dimensional subsonic wind tunnel. AIAA-82-0187 (1982)
4. Ashill, P.R. and Weeks, D.J. An experimental investigation of the drag of thick supercritical airfoils. A progress report RAE TM(Aero)1765 (1978)